AGU PUBLICATIONS

JGR

Journal of Geophysical Research: Atmospheres

RESEARCH ARTICLE
10.1002/2014JD021610

Key Points:
- Better explanation for QBO modulation of MLT zonal winds
- Occurrence of MSEE well correlated with weak stratospheric westward winds
- Strong SSWs influence the MSEE

Correspondence to:
G. Kishore Kumar,
kishoreg@rish.kyoto-u.ac.jp

Citation:
Kishore Kumar, G., K. Kishore Kumar, W. Singer, C. Zülicke, S. Gurubaran, G. Baumgarten, G. Ramkumar, S. Sathishkumar, and M. Rapp (2014), Mesosphere and lower thermosphere zonal wind variations over low latitudes: Relation to local stratospheric zonal winds and global circulation anomalies, *J. Geophys. Res. Atmos.*, *119*, 5913–5927, doi:10.1002/2014JD021610.

Received 10 FEB 2014
Accepted 30 APR 2014
Accepted article online 5 MAY 2014
Published online 28 MAY 2014

Mesosphere and lower thermosphere zonal wind variations over low latitudes: Relation to local stratospheric zonal winds and global circulation anomalies

G. Kishore Kumar[1,2], K. Kishore Kumar[3], W. Singer[1], C. Zülicke[1], S. Gurubaran[4], G. Baumgarten[1], G. Ramkumar[3], S. Sathishkumar[5], and M. Rapp[6]

[1]Leibniz-Institute of Atmospheric Physics e.V. at the Rostock University, Kühlungsborn, Germany, [2]Now at Research Institute for Sustainable Humanosphere (RISH), Kyoto University, Uji, Japan, [3]Space Physics Laboratory, Vikram Sarabhai Space Center, Trivandrum, Kerala, India, [4]Indian Institute of Geomagnetism, Navi Mumbai, India, [5]Equatorial Geophysical Research Laboratory, Indian Institute of Geomagnetism, Tirunelveli, India, [6]German Aerospace Center Institute of Atmospheric Physics (IPA), Oberpfaffenhofen, Wessling, Germany

Abstract Long-term observations from medium-frequency and meteor radars (1993–2012) and rocket soundings (1979–1990 and 2002–2007) are used to study mesosphere and lower thermosphere (MLT) zonal wind variations in relation to the stratospheric winds over northern low latitudes. The combined data set provides a complete height profile of amplitude of semiannual oscillation (SAO) up to 100 km, with an exception around 75–80 km. The SAO signal has maxima around 50 km and 82 km and a minimum around 65 km. The MLT zonal winds show remarkable interannual variability during northern hemispheric spring equinox and much less during fall equinox. Zonal wind mesospheric spring equinox enhancements (MSEE) appear with a periodicity of 2–3 years, suggesting a modulation by the quasi-biennial oscillation, which we identified with the strength of stratospheric westward winds. Out of 20 years of observations, the stratospheric westward winds are strong during 11 years (non-MSEE) and weak during 9 years. Six of these 9 years show large MLT winds (MSEE), and 3 years (1999, 2004, and 2006) show small MLT winds (missing MSEE). These unexpected small winds occur in years with global circulation anomalies associated with strong sudden stratospheric warmings and an early spring transition of zonal winds. With the proposed three MSEE classes, we take into account local and global forcing factors.

1. Introduction

The mesosphere and lower thermosphere (MLT) region is an important region of the Earth's middle atmosphere, where waves and their dissipation play a vital role for the energetics and dynamics. Small-scale turbulence to large-scale waves influence the dynamics of this region [*Fritts and Alexander*, 2003; *Baldwin et al.*, 2001]. Over tropical latitudes, the middle atmosphere is characterized by two distinct oscillations, namely, the semiannual oscillation (SAO) and the quasi-biennial oscillation (QBO).

SAO, the strongest mode of intraannual variability in the tropical middle atmosphere, was first observed in stratospheric zonal winds [*Reed*, 1966] with maximum amplitudes at the stratopause and is known as the stratospheric semiannual oscillation (SSAO). Subsequent studies [*Groves*, 1972; *Hirota*, 1980] using rocketsonde observations revealed that the amplitude of the SAO drops to a minimum at 65 km and reaches a secondary maximum at upper mesospheric heights that is known as mesospheric semiannual oscillation (MSAO). The SSAO and MSAO are out of phase with each other. The SSAO (MSAO) is characterized by eastward (westward) winds during equinoxes and westward (eastward) winds during solstices. Both SSAO and MSAO show a seasonal asymmetry with stronger zonal wind variations during the first cycle [*Delisi and Dunkerton*, 1988; *Garcia et al.*, 1997]. The asymmetry between the two cycles of the semiannual oscillation is ascribed to differences in the extratropical planetary wave forcing. The source of the SSAO is thought to be both meridional advection and eddy momentum deposition by internal gravity waves (GWs) and planetary waves [*Andrews et al.*, 1987]. Vertically propagating waves interact with the mean flow and deposit their momentum in the upper stratosphere. While the forcing of SSAO through wave contributions is well established and has been discussed extensively [*Hitchman and Leovy*, 1988; *Hamilton et al.*, 1995; *Sassi and Garcia*, 1997], the forcing of the MSAO is not yet clear.

In general, the MSAO is considered as a wave-driven oscillation, and the forcing of the MSAO is attributed to a broad spectrum of vertically propagating GWs and high-speed Kelvin waves excited in the lower atmosphere [*Dunkerton*, 1982; *Sassi and Garcia*, 1997; *Richter and Garcia*, 2006]. The transmission of these waves to the mesosphere is controlled by the mean zonal wind of the SSAO, which allows the transmission of only those waves with opposite horizontal propagation direction with respect to the zonal wind direction. However, waves with horizontal phase velocity greater than the background zonal winds can also propagate into the mesosphere. The selective transmission of waves from stratosphere to mesosphere accounts for the phase shift between the SSAO and MSAO [*Dunkerton*, 1982; *Hitchman and Leovy*, 1986]. Recent observations by *Antonita et al.* [2008] revealed that the forcing owing to the short-period (less than 2–3 h) GWs are on the order of ~20–60% and ~30–70%, for the eastward and westward phases of MSAO, respectively. In addition to the zonal winds, the MSAO signature is also observed in tropical temperature and in the occurrence frequency of low-latitude mesospheric radar echoes [*Kishore Kumar et al.*, 2007, 2008a, 2008b].

The QBO is predominantly seen in the tropical lower stratosphere with an approximate period of 27 months. It strongly controls the vertical coupling between lower and upper atmosphere over tropical latitudes. Although the QBO is a tropical phenomenon, it has a strong influence on the dynamics of extratropical latitudes [*Baldwin et al.*, 2001]. On one hand, the QBO influences the occurrence of sudden stratospheric warming (SSW) [*Holton and Tan*, 1980]. On the other hand, the SSW influences the tropical middle atmosphere and ionosphere [e.g., *Sathishkumar et al.*, 2009; *Pedatella and Liu*, 2013].

Besides the filtering of vertically propagating waves owing to the SSAO, the filtering owing to the stratospheric QBO (SQBO) affects the MLT winds. For the first time, *Burrage et al.* [1996] observed the influence of the SQBO on the MSAO in the zonal winds at tropical latitudes with High Resolution Doppler Imager observations. They found a striking variation in the strength of westward winds during March equinox (hereafter spring equinox) with a 2 year periodicity. Later ground-based observations and theoretical studies revealed the large mesospheric westward winds, which has been interpreted as mesospheric QBO (MQBO) [*Garcia et al.*, 1997; *Garcia and Sassi*, 1999; *Sridharan et al.*, 2007; *Ratnam et al.*, 2008; *Day and Mitchell*, 2013; *de Wit et al.*, 2013] and mesospheric quasi-biennial enhancement [*Venkateswara Rao et al.*, 2012a]. *Garcia and Sassi* [1999] used an equatorial beta plane model to demonstrate the influence of the mesospheric semiannual enhancement using tropical convection as a proxy for the wave source. They found that the enhancement is apparent during the MSAO westward phase and SQBO eastward phase and the convectively generated high-frequency GWs with horizontal phase speeds less than 40 ms^{-1} are responsible for the enhancement of the mesospheric winds. With the Hamburg model of the neutral and ionized atmosphere, a general circulation model, *Peña-Ortiz et al.* [2010] showed that the selective filtering of waves propagating through stratospheric winds can modulate the westward phase of the MSAO. Recently, *Ern et al.* [2014], using satellite observations, reported that the critical level filtering of gravity waves is the main process by which the SQBO affects the gravity wave spectrum. For this purpose, the authors investigated the gravity wave spectra, as well as the gravity wave variances and the momentum fluxes. Consequently, the range of wind speeds covered by the SQBO in the stratosphere, at a given time, should be a good proxy for the range of gravity wave phase speeds that cannot reach the MLT region during spring and fall equinoxes. Some studies also reported a SQBO influence on the MLT diurnal tides [*Vincent et al.*, 1998; *Hagan et al.*, 1999; *Mayr and Mengel*, 2005; *Xu et al.*, 2009].

The main aim of this paper is to study the MLT zonal wind variations over northern low latitudes in relation to the stratosphere. The present study has two parts. In the first part, we deal the relationship between MSAO and SSAO using long-term zonal wind observations from rocket soundings and radars at low latitudes around 8.5°N. In the second part, we discuss the interannual variability of the stratosphere and MLT zonal winds with focus on the enhancement in MLT westward winds during spring equinox in relation to the SQBO and SSW.

Section 2 describes the details of the database used: MLT winds from medium frequency (MF) radar and meteor radar (MR), rocket soundings, and Modern Era Retrospective analysis for Research and Applications (MERRA) winds. Section 3 discusses the composite monthly mean behavior of zonal winds over the study location, the interannual variability of stratospheric and MLT winds, and the influence of the stratospheric winds on the MLT winds. Section 4 provides the summary and conclusions.

2. Database and Analysis

2.1. Radar Observations of MLT Winds

Long-term zonal wind observations (1993–2009) by MF radar located at Tirunelveli, India (8.7°N, 77.8°E), were used. This radar operates at 1.98 MHz with a peak transmitter power of 25 kW and provides winds through spaced antenna analysis. The system details, mode of operation, and the method of wind determination can be found in *Rajaram and Gurubaran* [1998]. The winds are available with a vertical resolution of 2 km and with a temporal resolution of 2 min. Although the MF radar provides wind information in the altitude region 68–98 km, the data coverage in the lower height region below 80 km is limited. Therefore, only the data in the altitude region 80–98 km are used in this study. Two-minute wind values are used to estimate hourly winds. Those hourly winds are used for the composite wind analysis.

Additionally, the observations from the meteor radar (MR) located at Trivandrum, India (8.5°N, 77°E), over the period June 2004 to May 2012 were included. This radar system operates at 35.25 MHz with a peak power of 40 kW. A special transmitting scheme has been worked out to avoid the echoes from the equatorial electrojet, a well-known *E* region phenomenon in the equatorial ionosphere [*Kumar et al.*, 2007]. Wind profiles from MR are derived based on the interferometric technique. The meteors detected at zenith angles between 10° and 60° are used to estimate the winds. We estimated hourly winds in six height bins viz., 82, 85, 88, 91, 94, and 98 km. Those hourly winds are used for the composite wind analysis. We used two kinds of composite analyses to get winds, namely, a monthly composite and a 10 day composite shifted by 5 days (10 day/5 day). Differences over various composite analyses can be found in *Kishore Kumar et al.* [2014].

For monthly composite winds, first, the diurnal composite winds are compiled based on the hourly winds from the MF radar and the meteor radial velocities from the MR over a month. Then we apply a least squares fit analysis to extract mean 24 h, 12 h, and 8 h components. The mean winds are almost free from the tidal influence. For the 10 day composite winds, the estimation of the mean winds and tidal components is done by forming diurnal composite winds based on 10 day observations. The estimated winds are assigned to the sixth day; to calculate the next point, we shifted the composite window by 5 days.

The mean winds were also assessed by averaging the hourly winds over a month and over 10 day shifting by 5 days as discussed earlier. These comparisons confirmed that the mean winds obtained from both methods are robust and in good agreement. Further, to improve the quality of the data set, we considered only those months where more than 10 days of observations were available for calculating the monthly means. The monthly mean winds are then used to study interannual variability, and the 10 day composite winds are used to study the temporal variability.

2.2. Rocket Soundings

We use rocket soundings carried out at Thumba Equatorial Rocket Launching Station, Trivandrum, India (8.5°N, 76.9°E), during the Indian Middle Atmosphere Program (IMAP) and the Middle Atmospheric Dynamics Program-MIDAS (see details in *Kishore Kumar et al.* [2008a] and *Ramkumar et al.* [2006], respectively). Soviet meteorological M-100 rocketsondes were used for wind measurements during the IMAP for the period 1971–1990 (nearly 700 soundings), and Rohini sounding rockets (RH-200) were used during the MIDAS program for the period November 2002 to November 2007 (146 soundings). Horizontal winds with a height resolution of 1 km are available. The upper boundary for M-100 varies from 70 to 80 km, depending on the background conditions, whereas for RH-200 sounding it is 65 km. The standard errors involved in the RH-200 derived winds are 2.7 ms^{-1} in the altitude region 20–30 km, 1.9 ms^{-1} in the altitude region 31–50 km, and 3.8 ms^{-1} in the altitude region 50–55 km [*Devarajan et al.*, 1984].

2.3. MERRA Winds

MERRA winds are a product of NASA's Global Modeling and Assimilation Office (GMAO) atmospheric global reanalysis project. MERRA uses a three-dimensional variational data assimilation analysis algorithm based on the Gridpoint Statistical Interpolation scheme. The assimilation system utilizes the Goddard Earth Observing System model, version 5. The MERRA time period covers the modern era of remotely sensed data, from 1979 through the present, and the special focus of the atmospheric assimilation is the hydrological cycle [*Rienecker et al.*, 2011]. For this study, we utilized the direct analyzed product with a short name

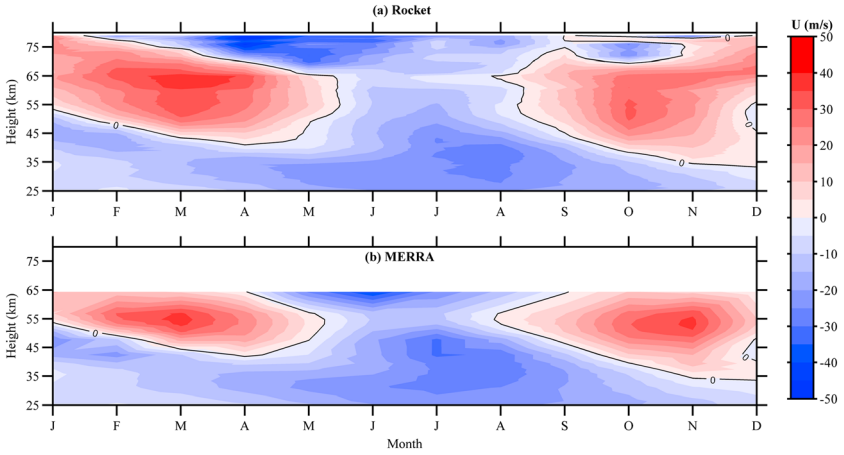

Figure 1. Composite monthly mean (a) zonal winds from rocket soundings (1971–1990 and 2002–2007) and (b) zonal mean zonal winds from MERRA (1993–2012) over Trivandrum.

MAI6NPANA that has a native (0.67° longitude × 0.5° latitude) horizontal resolution, 6 h time resolution, and is analyzed at standard vertical pressure levels (42 levels from 1000 hPa to 0.1 hPa).

The comparison of MERRA winds with correlative rocket soundings during the MIDAS program reveals both positive and negative biases. In general, the absolute biases are less than 6 ms^{-1}; however, occasionally, the biases are spread to 10–13 ms^{-1} in the altitude region 30–50 km, and 5–20 ms^{-1} in the altitude region 50–60 km, with large bias during early winter and early summer months. Very large biases are observed at 0.1 hPa. Several factors influence these biases in MERRA like the inadequate temperature observations and the background dynamics. The weak temperature gradients and the vertical averaging caused by the thick weighting functions associated with nadir radiance observations, as well as the lack of accurate balance constraints between winds and temperature fields in the tropics, lead to large biases in MERRA winds [*Rienecker et al.*, 2011].

Additional data sets, which are used to substantiate the background wind influence, are Singapore (1.36°N, 103.98°E) radiosonde observations and Free University Berlin (FUB) QBO winds (http://www.geo.fu-berlin.de/en/met/ag/strat/produkte/qbo/). Note that in the entire paper, four seasons are used. The corresponding months for each season are November, December, January, and February for winter; March and April for spring equinox; May, June, July, and August for summer; and September and October for fall equinox.

3. Results and Discussion

3.1. Composite Monthly Mean Zonal Winds

Our studies start with a brief description of the middle atmospheric zonal winds prevailing over the study region. Figures 1a and 1b illustrate the climatological monthly mean zonal winds estimated from the rocket observations over Thumba, India, and MERRA zonal mean zonal winds over 8.5°N, respectively. Note that the rocket observations during the IMAP (1971–1990) and MIDAS (November 2002 to November 2007) campaigns are averaged to get the climatological monthly mean winds. MERRA winds for the period 1993–2012 are used to extract the composite zonal mean winds. We estimated the difference between zonal mean zonal wind and zonal wind over Thumba (77.3°E) longitude from the MERRA and are about 2–5 ms^{-1}. In general, the prevailing zonal wind shows similar patterns in observations and reanalysis winds with slight differences in magnitude. These differences could be due to biases in MERRA winds as discussed in section 2.3 and also data length and period used for extracting the mean winds. The background wind system in Figure 1 evidently shows a distinct variation with height. Below 40 km, the background zonal wind is dominated by westward flow throughout the year, an exception during November and December in the height region of 35–40 km. Above 40 km, the background zonal wind shows semiannual variability that is more prominent around 50 km and again above 70 km. Around 50 km, the background zonal wind is eastward during equinoxes and westward during solstices (SSAO). Above 70 km, the background zonal wind is westward during equinoxes and eastward during solstices (MSAO).

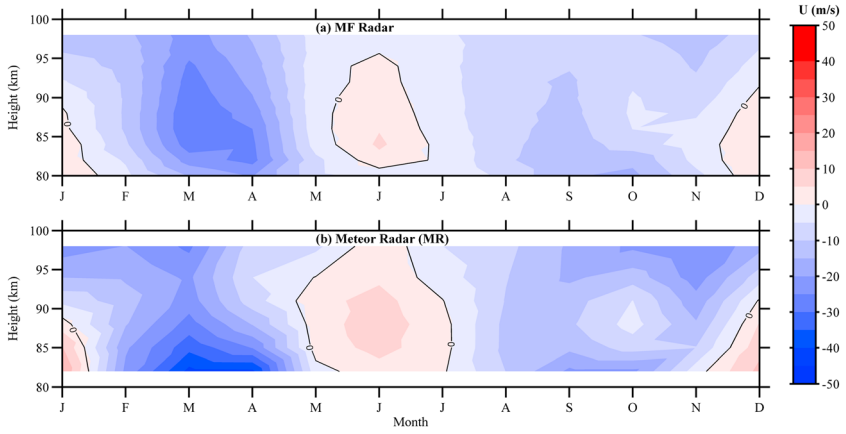

Figure 2. Composite monthly mean zonal winds from (a) MF radar (1993–2009) and (b) meteor radar (2004–2012).

The composite monthly mean zonal winds derived from MF radar observations (1993–2009) and MR observations (2004–2012) are illustrated in Figures 2a and 2b, respectively. The composite mean zonal winds from MF radar and MR observations show similar patterns with slight differences in magnitude. MF radar winds are smaller than the MR winds. The differences in the winds can be attributed to the differences of the observational technique, as reported previously by *Gurubaran et al.* [2008]. Below 90 km, both observations reveal a strong semiannual oscillation with westward winds during equinoxes and eastward winds during solstices. Above 90 km, the zonal wind is mostly dominated by westward wind owing to the tidal momentum deposition. Note that the first cycle of the MSAO is stronger than the second cycle, as documented in previous observations in the tropical middle atmosphere [*Garcia et al.*, 1997; *Rajaram and Gurubaran*, 1998; *Kishore Kumar et al.*, 2008a]. The strength of the spring equinox zonal wind is twice the strength of the fall equinox zonal wind, as observed earlier over nearby latitudes [*Kishore Kumar et al.*, 2008a].

We applied a least squares fit with periods 6 and 12 months to the composite monthly mean zonal winds (Figures 1 and 2) to extract the semiannual and annual components, respectively. Figures 3a and 3b show the amplitudes of semiannual and annual components. Although the winds from rocket soundings are partly available up to 80 km, we confined the estimation of SAO and annual oscillation (AO) amplitude up to 75 km

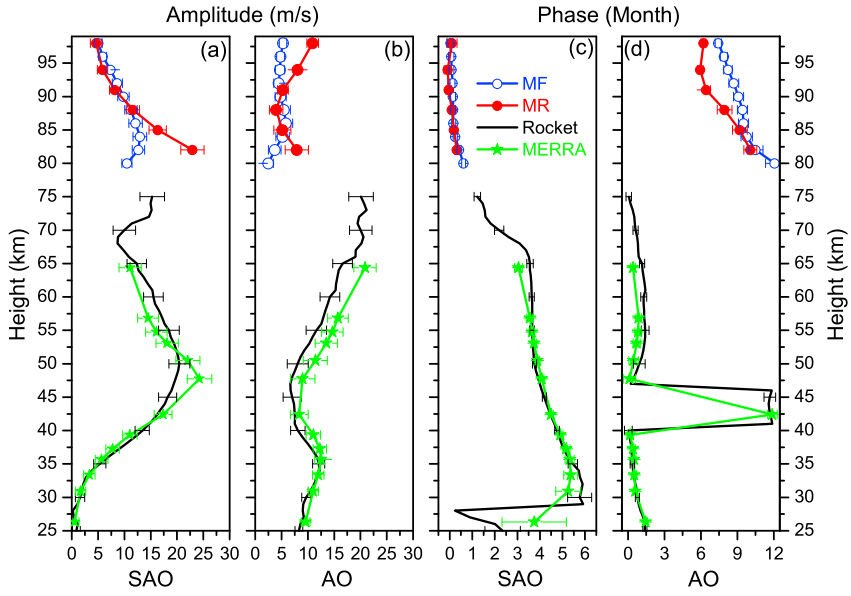

Figure 3. Height profiles of (a) semiannual amplitude and (b) annual amplitude from rocket, MERRA, MF, and meteor radar winds. (c and d) Same as Figures 3a and 3b but for phase (time of the maximum eastward component) profiles.

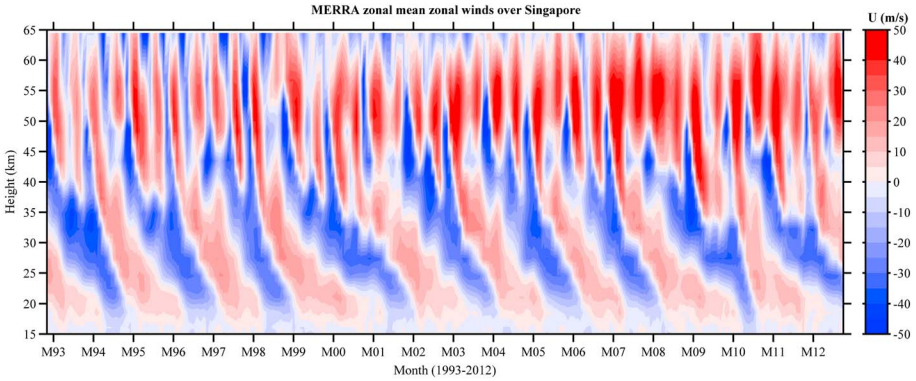

Figure 4. Height-time variation of zonal mean zonal winds over Singapore from MERRA. Note that "M93" stands for March 1993 and "M94" stands for March 1994 and so on.

owing to limited coverage and the limitations of rocket soundings. The stratospheric SAO and AO amplitudes are consistent in the rocket soundings and MERRA with slight differences in magnitude. The amplitude differences could be attributed to biases in reanalysis winds as discussed in section 2.3 and to the length of the data series. The mesospheric SAO and AO from MF radar and MR observations show different amplitudes. The observed differences could also be attributed to the interannual variability of the mean winds or to the data interval. *Venkateswara Rao et al.* [2012a] noticed a large interannual variability in mesospheric SAO and AO amplitudes over different tropical latitudes. We discuss the interannual variability of MLT winds in the next section. Salient features of the MSAO such as peak amplitudes around 82 km and a decrease with height above 82 km are consistent with previous observations [*Kumar et al.*, 2011; *Venkateswara Rao et al.*, 2012a].

The phase profiles of semiannual and annual components are shown in Figures 3c and 3d. Here the phase is defined as the time of maximum eastward component. The phase of SAO shows clear downward phase propagation. These profiles are in agreement with earlier observations [*Hirota*, 1980]. The phase difference between SSAO and MSAO clearly indicate the out-of-phase relationship between them. The phase difference between rocket and MERRA, below 35 km, might be influenced by the QBO winds. The different time spans of the data could be the responsible for the phase differences. The phase jump in the AO at 40–45 km both in MERRA and in the rocket data could be related to direct ozone heating.

In summary, the SAO peaks around 50 km and around 82 km with a minimum around 65 km. The SAO amplitudes are in agreement with *Baldwin et al.* [2001] (refer to Figure 30 of this article) based on the rocket observations from Ascension Island (8°S, 14°W), which is a nearly conjugate latitude to the study location. The AO amplitudes are larger in the height region 55–75 km and show different behavior at MLT heights compared to that of *Baldwin et al.* [2001]. It is worth to mention that the observed amplitude and phase profiles are in good agreement with the satellite observations of zonal mean temperatures [*Xu et al.*, 2007]. Thus, Figures 1, 2, and 3 describe the mean zonal wind characteristics in the stratosphere and MLT over the study region.

3.2. Interannual Variability of Stratosphere and MLT Zonal Winds

In this section, we discuss the interannual variability of the zonal winds in the stratosphere and MLT. The effects of mean winds are crucial for the propagation of GW that originated in the lower atmosphere. Winds in the troposphere and stratosphere provide a directional and speed filter. Thus, sharply, it limits the phase speeds of waves capable of reaching the upper mesosphere. Over tropical latitudes, the SQBO has a high impact on the MLT through the selective transmission of GWs. Recent satellite observations by *Ern et al.* [2014] showed critical level filtering by the SQBO on the transmission of GWs from the lower atmosphere. So first, we discuss the interannual variability of the stratospheric winds during the period 1993–2012.

In general, the radiosonde observations over Singapore are used as a proxy for stratospheric behavior and provide zonal wind information up to 5 hPa (~35 km). In order to extend zonal wind information to higher altitudes, we used MERRA winds over Singapore latitude, bearing in mind the bias in reanalysis winds as discussed in section 2.3. Figure 4 illustrates a time-height cross section of MERRA zonal mean zonal winds for the period 1993–2012 for the latitude of Singapore. The figure shows the characteristic descending phase of the stratospheric QBO below 40 km as reported earlier [e.g., *Baldwin et al.*, 2001]. Above 40 km, the wind

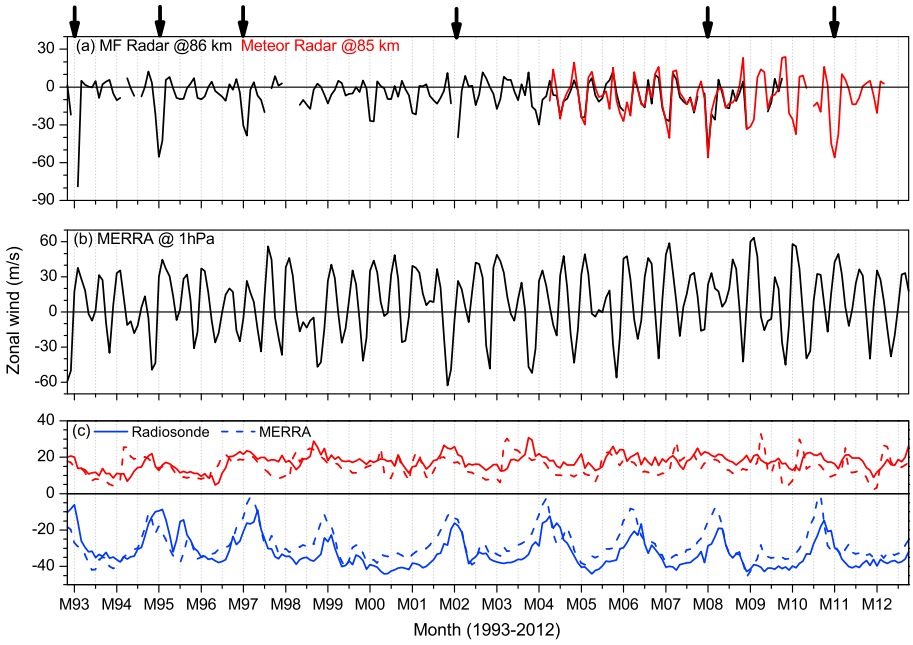

Figure 5. Temporal variation of (a) monthly mean zonal winds from MF radar (86 km) and meteor radar (85 km), (b) monthly zonal mean zonal winds at 1 hPa from MERRA, and (c) strongest stratospheric westward winds and strongest stratospheric eastward winds from Singapore radiosonde observations (solid lines) and MERRA (dashed lines). The arrows indicate the MSEE years. Details are given in the text.

pattern shows a seasonal variability corresponding to the SSAO with strong eastward wind during equinoxes and westward winds during solstices, similar to Figure 1. A systematic descending tendency of the SSAO eastward phase to continue into SQBO eastward phase is also visible. One can notice the strong interannual variability in the stratospheric winds from Figure 4. This interannual variability will alter the propagation conditions for the waves from the lower atmosphere, implying an interannual variability at MLT heights.

Furthermore, to illustrate how the interannual variability of stratospheric winds influences the MLT winds, the monthly mean strongest westward winds and eastward winds (hereafter stratospheric westward winds and eastward winds, respectively) were calculated in the region of 100 hPa to 5 hPa (~16 to 35 km) from Singapore radiosonde observations and MERRA winds (Figure 5c). In general, the stratospheric westward winds show a strong interannual variability, and small magnitudes are found around spring equinox months during selective years. The occurrence of small magnitudes shows a cyclic behavior with a period of 2–3 years. This periodicity is due to the QBO present at this height region. MERRA winds also reproduce the observed features in radiosonde winds but are offset from the Singapore radiosonde winds. The MERRA zonal winds at 1 hPa (proxy for SSAO) are shown in Figure 5b.

The monthly mean zonal winds observed with the MF radar (at 86 km) and the MR (at 85 km) are illustrated in Figure 5a. Although there are small differences in the wind amplitudes of the MF radar and the MR observations, they show good consistency during the overlapping period. The MSAO with westward winds during equinoxes and eastward winds during solstices is clearly evident in all years. Substantial interannual variability is also found in the MSAO. Note that the MLT westward winds show large interannual variability mainly during spring equinox, while the MLT westward winds during fall equinox and eastward winds during solstices show much less interannual variability. The observed peak westward winds are ~90 ms^{-1}, ~65 ms^{-1}, ~52 ms^{-1}, ~92 ms^{-1}, ~72 ms^{-1}, and ~62 ms^{-1} during the spring equinoxes of 1993, 1995, 1997, 2002, 2008, and 2011, respectively. For the other years, the peak westward winds during spring equinox are about 40 ms^{-1}.

The zonal winds at 1 hPa (~50 km) (SSAO) and MLT zonal winds at 85 km (MSAO) are in opposite phase. Furthermore, the large westward MLT winds during spring equinox seem to coincide with the weak stratospheric westward winds, but not all the years with weak stratospheric westward winds have large westward winds in the MLT. The observed large westward MLT winds have a systematic periodicity (2–3 years)

during certain periods (1993–2002 and 2008–2011). These large westward winds have been interpreted as MQBO. *Garcia and Sassi* [1999] reported that the SQBO modulates the MLT winds through selective filtering of the spectrum of vertically propagating westward GWs forced by deep convection in the tropics.

Several studies [e.g., *Burrage et al.*, 1996; *Garcia et al.*, 1997; *Sridharan et al.*, 2007] tried to explain the connection between SQBO and MQBO, but this remained a hypothesis because of the paucity of observations. *Ratnam et al.* [2008] showed that the relationship between SQBO and MQBO varies with time in the height region 70–80 km. However, the data used for this study had limited coverage, so the results might have aliasing effects from the diurnal tide [*Smith*, 2012]. The present observations do not have such time constraints, and the mean winds are almost free from a tidal contamination. Moreover, long-term observations (~20 years) give us the possibility to study the SQBO modulation on MLT winds in more detail.

3.3. SQBO Modulation of MLT Zonal Winds

In general, two approaches are followed to study the SQBO modulation of MLT winds. The first approach is based on the SQBO phase, which is defined based on the monthly mean zonal winds at a reference pressure level either 10 hPa, 30 hPa, or 50 hPa [e.g., *Vincent et al.*, 1998; *Sridharan et al.*, 2007; *Peña-Ortiz et al.*, 2010; *de Wit et al.*, 2013]. The second approach is based on the zonal wind strength in the region of 100 hPa to 10 hPa (~16 to 32 km) [e.g., *Garcia et al.*, 1997]. With the first approach, one can get a correlation between the SQBO phase and MLT changes, but this approach cannot provide a mechanism linking SQBO and MLT winds. The second approach could help to discriminate the GW propagation conditions and possible influences on the MLT changes. Both approaches are applied to our data, and we discuss the possible differences. As no significant differences were noted between monthly and seasonal scales, we discuss the SQBO modulation on seasonal basis.

To examine the seasonal tendency of the SQBO modulation, the data were grouped into four seasons. For each season, the peak MLT winds at 85 km are compared with different SQBO proxies such as the mean winds at 10 hPa and 50 hPa from FUB QBO winds and the stratospheric westward winds from Singapore radiosonde observations. Figure 6 illustrates the comparisons during spring and fall equinoxes.

Based on the scatterplots (Figures 6a–6d), the variation of MLT winds with respect to 10 hPa or 50 hPa winds does not show any specific relation during both spring and fall equinoxes. Earlier observations reported large westward MLT winds during SQBO eastward phase, as the eastward phase of SQBO will allow the westward propagating GWs that in turn produce large MLT winds [*Burrage et al.*, 1996; *Sridharan et al.*, 2007; *Peña-Ortiz et al.*, 2010]. Since the SQBO phase changes significantly with respect to the pressure level, the selection criterion is highly sensitive to the reference pressure level. This is clearly evident in the scatterplots for 10 hPa and 50 hPa (Figures 6a and 6c). Further, not all the years during SQBO eastward phase have large MLT winds. This is true for both pressure levels.

In contrast, the MLT data set during spring equinox can be grouped into two categories based on the stratospheric westward winds (Figure 6e). In years with large stratospheric westward winds, the range of observed MLT winds is small. In years with small stratospheric westward winds, however, the MLT winds tend to be distributed over a wide range. Moreover, this distribution can be categorized into two subgroups, one with large MLT winds and another with relatively small MLT winds.

From the scatterplots (Figure 6), clearly the approach based on SQBO phase at a given pressure level cannot provide any conclusive association between MLT and stratospheric winds, while the strongest westward wind approach provides a reasonable association between the two. In general, the weak stratospheric westward winds will allow a larger flux of westward propagating GWs to the mesosphere, where these waves deposit westward momentum and thus drive the large westward winds at MLT altitudes. Thus, the strength of the stratospheric westward winds may explain the strength of the MLT westward winds.

During the fall equinox, the MLT winds are not as large as during spring equinox. This could be explained based on the strength of stratospheric westward winds. In general, the stratospheric westward winds are large during the fall equinox (Figure 6f), which limits the flux of westward propagating waves transmitted to the MLT. Further, the stratospheric westward winds during the fall equinox do not show any considerable interannual variability as noted during spring equinox months. Although the SAO is in the same phase at both equinoxes, the influence of the stratospheric westward wind is stronger in the spring equinox than in the fall equinox, because it usually peaks in early summer. This may result in weaker MLT winds during fall

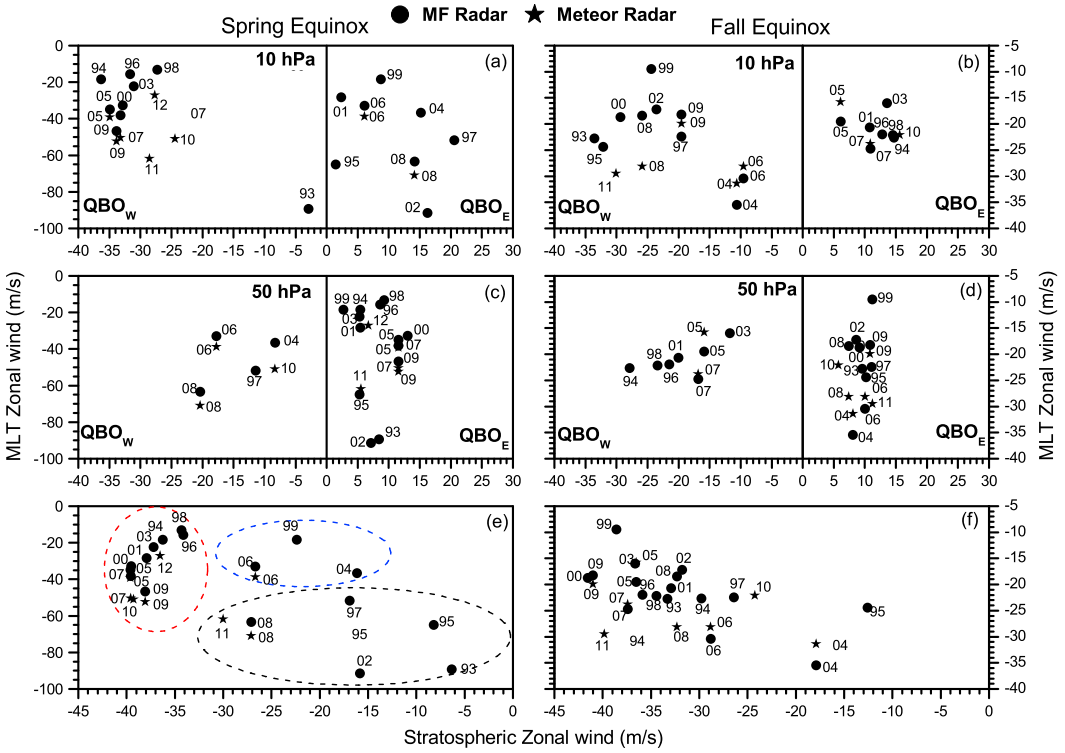

Figure 6. Scatterplots of peak MLT winds at 86 km from MF radar and at 85 km from MR against mean winds at 10 hPa from FUB QBO data during (a) spring equinox and (b) fall equinox. (c and d) Same as Figures 6a and 6b but with mean winds at 50 hPa from FUB QBO data. (e and f) Same as Figures 6a and 6b but for the strongest stratospheric westward winds. Please note the different *x* axis scaling. Note that the MF radar observations are depicted by filled circle symbols and MR observations by filled star symbols. The numbers in the scatterplots represent the year. MSEE, non-MSEE, and missing MSEE are indicated with dashed ellipses.

equinox and a relatively weak interannual variability. Similarly, winter and summer seasons also do not show any considerable interannual variability in association with stratospheric winds. Earlier observations [*Garcia et al.*, 1997; *Sridharan et al.*, 2007] also reported that the QBO influence is large for the westward winds at MLT and confined to spring equinox.

Because we found most variability of MLT winds during spring equinox, including extreme winds, we name these mesospheric spring equinox enhancements (MSEE) in order to separate these from the less variable fall equinox event. Based on the scatterplots during the spring equinox (Figure 6e), the MLT winds are categorized into three groups as follows: (1) non-MSEE: strong stratospheric westward winds with weak MLT westward winds (the most general behavior), (2) MSEE: weak stratospheric westward winds with strong MLT westward winds, and (3) missing MSEE: weak stratospheric westward winds with weak MLT westward winds. Only three cases belong to this group. It is worth to mention that the MSEE years are not the exceptional cases, since they belong to the expected anticorrelation between stratospheric winds and mesospheric winds. The missing MSEE years instead are outliers from this anticorrelation, and therefore, these years are termed "anomalous" years.

To illustrate the temporal variability of MLT winds for the three groups, we calculated the mean values of zonal winds for each group by using the 10 day/5 day composite winds using MF radar and MR separately (Figure 7). The important observations from Figure 7 are as follows:

1. A systematic temporal variation with a gradual increase and decrease in the westward flow during spring equinox months is observed.
2. Large westward winds are observed during spring equinox months with peak values around day 80 for the MSEE. This is attributed to the weak stratospheric westward winds during the MSEE.
3. The transition from eastward to westward is noted during late January for non-MSEE and MSEE. But for missing MSEE, the transition takes place during early January.

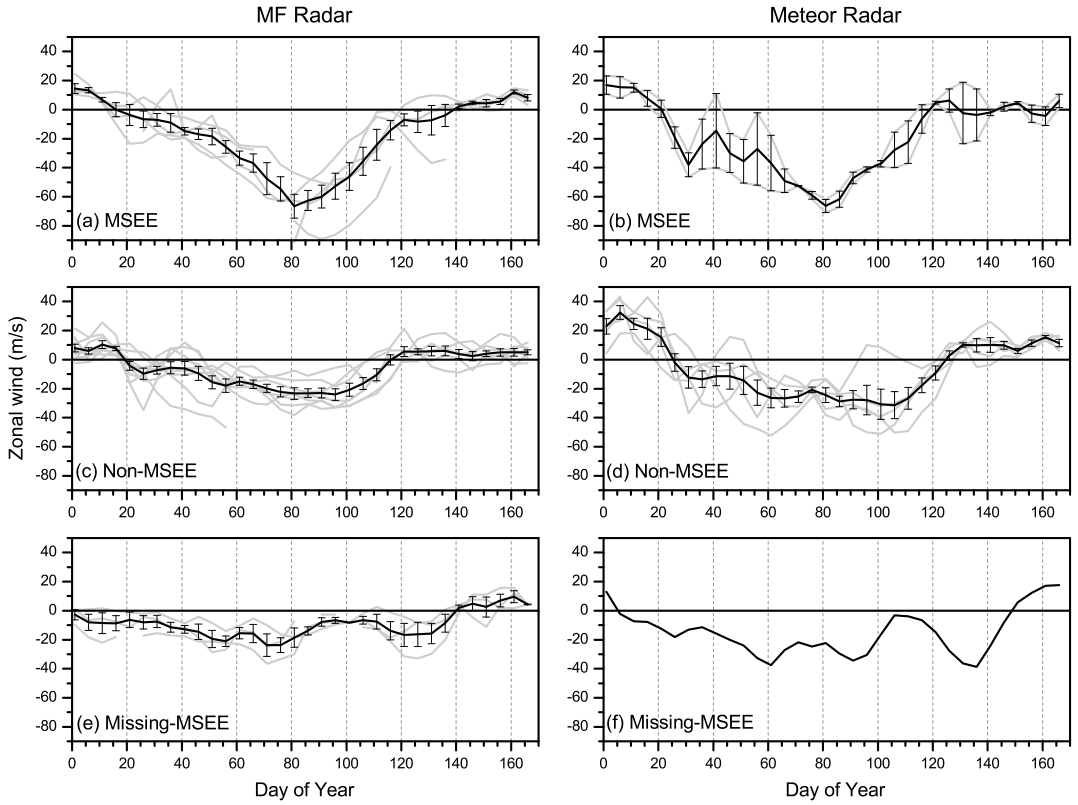

Figure 7. Temporal variation of climatological mean values of zonal winds derived from 10 day/5 day analysis for MSEE, non-MSEE, and missing MSEE: (a, c, and d) at 86 km from MF radar (1993–2009) and (b, d, and e) at 85 km from meteor radar (2004–2012). The error bar stands for the standard error. The gray lines stand for individual years.

To investigate the influence of eastward to westward transition, at 86 km for MF radar and at 85 km for MR, during winter on the spring equinox winds, we compared the January monthly mean winds with peak westward winds during spring equinox (figure not shown). From this comparison, it is clear that the monthly mean zonal wind during January is eastward in general and westward only during selective years. It is noteworthy to mention that these years was related to the missing MSEE. We observed that the zonal winds became westward during early January and that feature propagates downward as a function of time. Thus, filtering of the westward waves may take place at lower heights than the observational window. This implies less westward momentum, and therefore, MSEE is missing during these years.

A classification of MSEE events is given in Table 1. Based on the stratospheric westward winds during the spring equinox, we term those conditions favorable if the zonal wind is weaker than $-31\ \mathrm{ms}^{-1}$. This well captures the QBO impact during the spring equinox. It appears from the data that the nonfavorable conditions in all cases resulted in non-MSEE. As noted above, not all favorable stratospheric conditions resulted in an MSEE event; the onset of spring transition could also influence the presence of MSEE. We used the zonal wind for January at 85 km as a proxy for the onset of spring transition. While it is above $0.5\ \mathrm{ms}^{-1}$ in normal winters, in some winters, it is already below this value indicating an early spring transition from eastward to westward wind. It turned out that the early spring transition was also related to the missing MSEE when the stratospheric conditions were favorable. *Sathishkumar et al.* [2009] reported changes in the winter zonal flow over Tirunelveli from eastward to westward during the years 1998–1999, 2003–2004, and 2005–2006. This has been explained by the variability of gravity waves in relation to the circulation changes associated with high-latitude SSW events. This coincidence is tempting us to speculate that the SSW could influence the MSEE. So we investigated MSEE classification in relation to SSW. For that purpose, we compiled a number of characteristics from *Tomikawa* [2010] and found the SSW intensity, the product of the number of days the westward wind at 10 hPa and 60°N and the peak westward wind to be suitable to distinguish strong ($I_{max} > 100\ \mathrm{ms}^{-1}$ d) from weak ($I_{max} < 100\ \mathrm{ms}^{-1}$ d) SSW events. We note that only the

Journal of Geophysical Research: Atmospheres

10.1002/2014JD021610

Table 1. Classification of MSEE Events[a]

	Strongest Stratospheric Westward Winds		Stratospheric Sudden Warmings (SSWs)					January Winds at 85 km		Spring Equinox Winds at 85 km	
Year	U (ms^{-1})	Flag	Central Date	Duration (days)	E_{max} (ms^{-1})	Intensity (ms^{-1} d)	Flag	U_{mean} (ms^{-1})	Flag	U_{peak} (ms^{-1})	Flag
1993	−6.3	F	--	--	--	--	--	1.5	N	−89.3	MSEE
1994	−36.3	NF	--	--	--	--	--	5.7	N	−18.33	non-MSEE
1995	−8.2	F	--	--	--	--	--	3.4	N	−64.92	MSEE
1996	−34.1	NF	--	--	--	--	--	7	N	−15.69	non-MSEE
1997	−16.9	F	--	--	--	--	--	6.4	N	−51.82	MSEE
1998	−34.3	NF	--	--	--	--	--	1.1	N	−13.2	non-MSEE
1999	−22.4	F	15 Dec 98	6	−23.7	142.2	S	0.2	E	−18.37	missing MSEE
			26 Feb 99	21	−19.3	405.3	S				
2000	−39.5	NF	20 Mar 00	3	−3.3	9.9	W	5.2	N	−32.73	non-MSEE
2001	−37.9	NF	11 Feb 01	13	−12.4	161.2	S	−1.7	E	−28.38	non-MSEE
2002	−15.9	F	31 Dec 01	3	−1.3	3.9	W	11	N	−91.5	MSEE
2003	−37.2	NF	18 Jan 03	1	−1.1	1.1	W	−0.1	E	−22.2	non-MSEE
2004	−16.1	F	7 Jan 04	9	−13.5	121.5	S	−15.6	E	−36.58	missing MSEE
2005	−39.6	NF	--	--	--	--	--	19.5	N	−39.1	non-MSEE
2006	−26.6	F	21 Jan 06	26	−24.1	626.6	S	−10.8	E	−38.7	missing MSEE
2007	−39.6	NF	24 Feb 07	4	−8	32	W	16.1	N	−50.3	non-MSEE
2008	−27.1	F	22 Feb 08	7	−13.3	93.1	W	4.5	N	−70.9	MSEE
			14 Mar 08	7	−5.6	39.2	W				
2009	−38.1	NF	24 Jan 09	30	−28.8	864	S	23.2	N	−52.3	non-MSEE
2010	−39.3	NF	9 Feb 10	3	−5.6	16.8	W	23.8	N	−51.0	non-MSEE
			24 Mar 10	3	−2.1	6.3	W				
2011	−30.7	F	--	--	--	--	--	1.7	N	−61.9	MSEE
2012	−36.8	NF	--	--	--	--	--	4.9	N	−27.2	non-MSEE

[a]Strongest stratospheric westward winds within the region 100 hPa–5 hPa (~16–35 km) are taken from the Singapore radiosonde observations (used in Figure 5c). Zonal winds above $-31\ ms^{-1}$ are flagged "favorable (F)" and below $-31\ ms^{-1}$ "not favorable (NF)." The information about sudden stratospheric warmings (SSWs) is taken from *Tomikawa* [2010]. Following this procedure, the data for 2010 have been calculated from ERA-Interim. Duration (D) represents the number of days with zonal mean westward wind at 10 hPa and 60°N; E_{max} indicates the maximum speed of the westward wind. Intensity (I_{max}), the product of D and E_{max}, less than 100 is indicative for "weak (W)" and above 100 "strong (S)" SSWs. January winds at 85 km were taken from MF radar observations for 1993–2004 and from MR observations for 2005–2012. We used these as an indicator for the onset of spring transition: winds larger than $0.5\ ms^{-1}$ indicate "normal (N)" and less than $0.5\ ms^{-1}$ "early (E)" dates of spring transition. The peak westward winds at 85 km during spring equinox are used to quantify the MSEE events. If these zonal winds are below $-50\ ms^{-1}$ (for MF radar observations) and $-55\ ms^{-1}$ (for MR observations), it is associated to the group "MSEE." If the wind is larger, it is a missing MSEE for F conditions and non-MSEE for NF conditions.

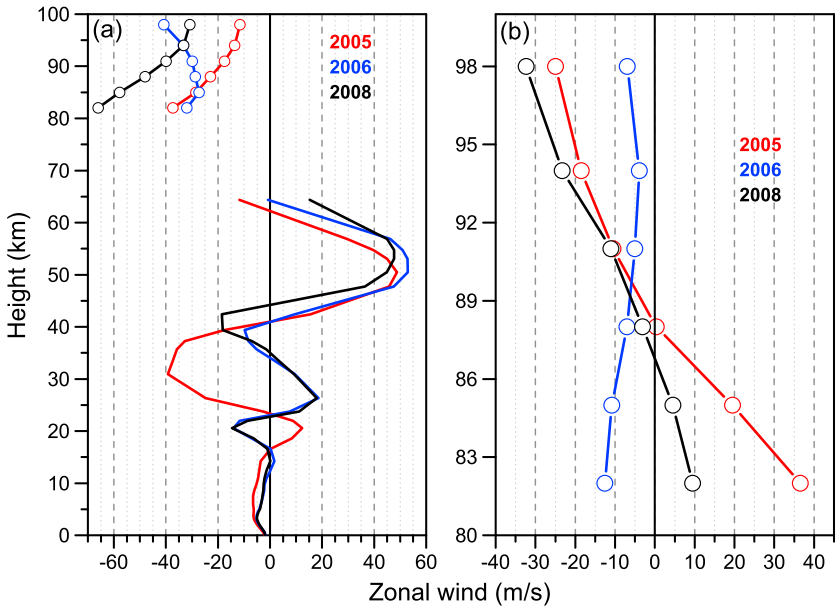

Figure 8. Height profiles of zonal winds, (a) averaged over the period day 70 to day 90 for selective years 2005 (non-MSEE), 2006 (missing MSEE), and 2008 (MSEE), lower part from MERRA and upper part from meteor radar observations. (b) January MLT winds for the years 2005, 2006, and 2008. Please note the different axis scaling.

strong events resulted in missing MSEE when the stratospheric conditions were favorable. It is worth to mention that strong SSW events are correlated with early transition during January, except the years 2003 and 2009. The first SSW was weak, but the spring onset was early, while the second SSW, one of the strongest SSWs reported [*Kuttippurath and Nikulin*, 2012], was associated with a normal transition. However, both cases appear in nonfavorable SQBO conditions and thus are irrelevant to the MSEE. An explicit study on the general influence of SSW on the tropical middle atmosphere goes well beyond the scope of the present study, and it needs further investigation.

3.4. Typical Examples of Different MSEE

Figure 8a shows zonal wind profiles constructed by averaging the daily zonal winds over the period from day 70 to day 90 for selected years 2005, 2006, and 2008. These years represent non-MSEE, missing MSEE, and MSEE, respectively. The MR observations are used for the MLT region and MERRA zonal winds over Singapore for lower heights. We regard the zonal winds from MERRA to be appropriate for discussion on a qualitative basis.

Following *Lindzen* [1981], during 2005, westward winds in the middle stratosphere with magnitudes of 40 ms^{-1} inhibit the propagation of westward GWs with smaller phase speeds, while during 2006 and 2008, westward GWs with phase speeds above 15–20 ms^{-1} can propagate to upper stratosphere. This leads to a relative enhancement in the flux of westward waves transmitted to the stratosphere during 2006 and 2008 when compared to 2005. Due to a reduced wave transmission to the MLT during 2005, the MLT winds are relatively small. On the other hand, the enhanced flux of westward waves during 2006 and 2008 could deposit more westward momentum in the MLT, which leads to an enhancement in westward winds. However, it is true if and only if no critical level is present between the upper stratosphere and the MLT.

In the mesosphere, we have an additional constraint due to the missing data between 65 and 82 km. We therefore extend our discussion by considering the variation of MLT zonal winds as a function of time. Figure 8b shows the MLT winds during January. From Figure 8b, one can notice that during January 2005 and 2008, the MLT winds are eastward, whereas in 2006, the zonal wind became westward during January. An early spring transition from eastward to westward during January 2006 may control the westward propagating waves to the observational height region (82–98 km). Possibly the westward waves may deposit their momentum at the lower height region, and this leads to a reduction in westward momentum transfer to the MLT. Recent observations by *Venkateswara Rao et al.* [2012b] showed less gravity wave variances at MLT heights during 2004 and 2006 compared to 2008.

In summary, the strongest stratospheric filtering is in 2005, consequently non-MSEE. While both 2006 and 2008 are associated with less filtering, 2008 is normal, and 2006 is abnormal. The enhanced flux of westward waves propagating from the lower atmosphere during 2008 leads to large westward winds, while during 2006, the early spring transition of zonal winds from eastward to westward may have lowered the critical level and lead to less westward momentum in the MLT region. Unfortunately, the region of potential GW breaking is not covered by our observations. There might be another possibility for the reduction of MLT winds during 2006 that is an anomalous cross-equator meridional circulation during the SSW years shifting the tropical momentum balance, resulting in weaker zonal winds. Maybe the anomalous circulation also could alter the temporal evolution of the winds in the MLT region from January to March.

4. Summary and Conclusions

Long-term wind observations by rocket soundings and radar observations are used to study the tropical semiannual oscillation (SAO) over northern low latitudes. The combination of these data provides a complete height profile of SAO amplitude from the stratosphere to the MLT, with a data gap around 75–80 km. Using nearly 2 decades of MLT observations, the interannual variability of MLT zonal winds are studied in relation to stratospheric winds. Our main findings are summarized as follows:

Clear seasonal variability is evident both in the stratosphere and mesosphere with opposite behavior. The stratosphere (mesosphere) shows semiannual variability with eastward (westward) wind during equinoxes and westward (eastward) wind during solstices. The first cycle of stratospheric SAO (SSAO) and mesospheric SAO (MSAO) is stronger than the second cycle as reported before. The height profile of SAO amplitude shows two distinct peaks around 50 km and 80 km, with a minimum around 65 km. The primary peak corresponds to SSAO, and the secondary peak corresponds to MSAO. The observed SAO amplitudes are consistent with the earlier observations of *Baldwin et al.* [2001]. The phase profiles of SAO show downward phase propagation, and the phase difference between stratosphere and mesosphere indicate out-of-phase relationship between SSAO and MSAO.

MLT winds from radar observations (1993–2012) show a remarkable interannual variability during the spring equinox and less interannual variability during the fall equinox. The interannual variability during the solstices is much less than the equinoxes. The spring equinox MLT westward winds show large magnitudes (termed MSEE) with a periodicity of 2–3 years. Further, the noticeable correlation between the strongest stratospheric westward winds in the region 100 hPa to 5 hPa (~16 to 35 km), and the MLT winds suggest that the spring equinox MLT westward winds are large when the stratospheric westward winds are weaker. In other words, the SQBO modulates the MLT westward winds during spring equinox.

From the investigation of 20 years of observations, the MLT winds during spring equinox are around climatological mean values (non-MSEE) in 11 years. This appeared during the years of strong stratospheric westward wind. The hypothesis that the weak stratospheric westward winds favor the appearance of MSEE could be confirmed for six cases (MSEE years). The underlying mechanism is a local forcing of the MLT region by gravity waves (GWs) due to less filtered westward waves enforcing large westward winds. Earlier observations relate the large MLT winds during spring equinox to the SQBO eastward phase, but the selection of the SQBO phase based on a single pressure level is error prone due to the high vertical variability of the SQBO. Although the correlation between the SQBO and the MLT winds is good, it does not hold all the time. That means not all the years with SQBO eastward phase have large MLT winds. Our explanation for large MLT winds in relation to the strongest stratospheric westward winds provides a conclusive association between the two. As an additional factor, we identified global circulation anomalies, which distinguish MSEEs from a local response to SQBO. The suggested classification is summarized as follows:

1. MSEE case: MSEE observed, SQBO favorable, SSW weak, or January wind normal.
2. Non MSEE case: MSEE not observed, SQBO unfavorable, and SSW and January wind irrelevant.
3. Missing MSEE case: MSEE not observed, SQBO favorable, SSW strong, or January wind early.

Further, the results are supported by the findings of *Garcia and Sassi* [1999] based on model simulations. Based on the numerical simulations of interactions between GWs and convection, *Eitzen and Randall* [2005] observed that the GWs with phase speeds of about 20 ms^{-1} deposit large westward momentum. Earlier observations [*Garcia et al.*, 1997; *Day and Mitchell*, 2013; *Venkateswara Rao et al.*, 2012a] also reported large

westward winds over different tropical latitudes. This indicates that the waves responsible for the MSEE are not limited to a localized wave source.

However, while the fall equinox MLT wind anomalies could well be explained with this hypothesis, three cases of spring equinox winds (missing MSEE years 2006, 2008, and 2011) could not and required further investigation. They could be linked to the presence of strong SSWs during these winters or, likewise, an early onset of the spring transitions. These anomalies in the global mesospheric circulation add to the local GW-related forcing. In these situations, the tropical westward wind band at MLT heights apparently is lowering and consequently favors the propagation of GWs with westward momentum to the MLT region. Unfortunately, we cannot investigate this hypothesis with the given data due to a gap between 60 (upper bound of MERRA) and 80 km (lower bound of radar). Also, modeling studies have to be reserved for future investigations because of the complex dynamics. The main drivers of global circulation anomalies during spring equinox are changes in heating conditions and unsteady dynamics of the polar vortex during winter. Its stability is relevant for the spring transition and has also consequences of Rossby wave dynamics, eddy fluxes, residual circulation and characteristic wind, and temperature patterns. The relevant processes depend on many factors. These have to be systematically varied in sequences of model runs. Hence, our study presents empirical evidence of local and global influences on the tropical MLT dynamics and poses a challenging task for further observational and modeling studies.

Meteor radar observations show the SQBO modulation of meridional diurnal tides with about 30% larger amplitudes during 2006, 2008, and 2011 compared to the other years [Kishore Kumar et al., 2014, personal communication], consistent with *Xu et al.* [2009] and *Mayr and Mengel* [2005]. The observed large diurnal tidal amplitudes support that GWs are responsible for the large MLT winds, which may interact with tides, and become responsible for the large tidal amplitudes. If this is true, then, the interannual variability of tidal amplitudes can be used as another tracer for a QBO modulation of the MLT. Further, it supports our explanation about westward momentum deposition at lower altitudes during missing MSEE years. However, other dynamical interactions of tides also need to be considered to make a concert decision, and a detailed study is needed to explore clear reasons.

The present study of radar, rocket, radiosonde, and reanalysis data gathered evidence for a local SAO and QBO modulation of MLT winds, which is especially strong in the variations during spring equinox. These MSEEs also show an association with winter global circulation anomalies, in terms of strong SSWs and early spring transitions. These processes also leave an imprint on tides, which in turn modulate the upper atmosphere. The detailed resolution of the relevant dynamics, which influence the low-latitude MLT region on local and global scales, is a challenging task for future studies.

Acknowledgments
The authors are grateful to Peter Hoffmann for helpful discussions. MERRA data used in this study have been provided by the Global Modeling and Assimilation Office (GMAO) at the NASA Goddard Space Flight Center through the NASA GES DISC online archive. G. Kishore Kumar acknowledges the Alexander von Humboldt Foundation, Germany, for support. We wish to thank three anonymous reviewers and the editor for their critical comments and suggestions that helped in bringing out this manuscript to the present stage.

References

Andrews, D. G., J. R. Holton, and C. B. Leovy (1987), *Middle Atmosphere Dynamics*, 489 pp., Academic, San Diego, Calif.
Antonita, T. M., G. Ramkumar, K. K. Kumar, and V. Deepa (2008), Meteor wind radar observations of gravity wave momentum fluxes and their forcing toward the Mesospheric Semiannual Oscillation, *J. Geophys. Res.*, *113*, D10115, doi:10.1029/2007JD009089.
Baldwin, M. P., et al. (2001), The quasi-biennial oscillation, *Rev. Geophys.*, *39*, 179–229, doi:10.1029/1999RG000073.
Burrage, M. D., R. A. Vincent, H. G. Mayr, W. R. Skinner, N. F. Arnold, and P. B. Hays (1996), Long-term variability of the equatorial middle atmosphere zonal wind, *J. Geophys. Res.*, *101*, 12,847–12,854, doi:10.1029/96JD00575.
Day, K. A., and N. J. Mitchell (2013), Mean winds in the MLT, the SQBO and MSAO over Ascension Island (8° S, 14° W), *Atmos. Chem. Phys.*, *13*, 9515–9523, doi:10.5194/acp-13-9515-2013.
Delisi, D. P., and T. J. Dunkerton (1988), Seasonal variation of the semiannual oscillation, *J. Atmos. Sci.*, *45*, 2772–2809.
Devarajan, M., P. R. Parameswaran, C. A. Reddy, and C. R. Reddy (1984), Accuracy of stratospheric wind measurements using chaff releases from RH-200 rockets, *Indian J. Radio Space Phys.*, *13*, 48–55.
de Wit, R. J., R. E. Hibbins, P. J. Espy, and N. J. Mitchell (2013), Interannual variability of mesopause zonal winds over Ascension Island: Coupling to the stratospheric QBO, *J. Geophys. Res. Atmos.*, *118*, 12,052–12,060, doi:10.1002/2013JD020203.
Dunkerton, T. J. (1982), Theory of the mesopause semiannual oscillation, *J. Atmos. Sci.*, *39*, 2681–2690, doi:10.1175/1520-0469(1982)039<2681:TOTMSO>2.0.CO;2.
Eitzen, Z. A., and D. A. Randall (2005), Numerical Simulations of Interactions between Gravity Waves and Deep Moist Convection, *J. Atmos. Sci.*, *62*, 1480–1496.
Ern, M., F. Ploeger, P. Preusse, J. C. Gille, L. J. Gray, S. Kalisch, M. G. Mlynczak, J. M. Russell III, and M. Riese (2014), Interaction of gravity waves with the QBO: A satellite perspective, *J. Geophys. Res. Atmos.*, *119*, 2329–2355, doi:10.1002/2013JD020731.
Fritts, D. C., and M. J. Alexander (2003), Gravity wave dynamics and effects in the middle atmosphere, *Rev. Geophys.*, *41*(1), 1003, doi:10.1029/2001RG000106.
Garcia, R. R., and F. Sassi (1999), Modulation of the mesospheric semiannual oscillation by the quasi-biennial oscillation, *Earth Planets Space*, *51*, 563–570.
Garcia, R. R., T. J. Dunkerton, R. S. Lieberman, and R. A. Vincent (1997), Climatology of the semiannual oscillation of the tropical middle atmosphere, *J. Geophys. Res.*, *102*, 26,019–26,032, doi:10.1029/97JD00207.

Groves, G. V. (1972), Annual and semi-annual zonal wind components and corresponding temperature and density variations, 60–130 km, *Planet. Space Sci.*, *20*, 2099–2112.
Gurubaran, S., D. Narayana Rao, G. Ramkumar, T. K. Ramkumar, G. Dutta, and B. V. Krishna Murthy (2008), First results from the CAWSES-India Tidal Campaign, *Ann. Geophys.*, *26*, 2323–2331, doi:10.5194/angeo-26-2323-2008.
Hagan, M. E., M. D. Burrage, J. M. Forbes, J. Hackney, W. J. Randel, and X. Zhang (1999), QBO effects in the diurnal tide in the upper atmosphere, *Earth Planets Space*, *51*, 571–578.
Hamilton, K., R. John Wilson, J. D. Mahlman, and L. J. Umscheid (1995), Climatology of the SKYHI troposphere stratosphere mesosphere general circulation model, *J. Atmos. Sci.*, *52*, 5–43, doi:10.1175/1520-0469(1995)052.
Hirota, I. (1980), Observational evidence of the semiannual oscillation in the tropical middle atmosphere–A review, *Pure Appl. Geophys.*, *118*, 217–238.
Hitchman, M. H., and C. B. Leovy (1986), Evolution of the zonal mean state in the equatorial middle atmosphere during October 1978–May 1979, *J. Atmos. Sci.*, *43*, 3159–3176.
Hitchman, M. H., and C. B. Leovy (1988), Estimation of the Kelvin wave contribution to the semiannual oscillation, *J. Atmos. Sci.*, *45*, 1462–1475.
Holton, J. R., and H. Tan (1980), The Influence of the Equatorial Quasi-Biennial Oscillation on the Global Circulation at 50 mb, *J. Atmos. Sci.*, *37*, 2200–2208.
Kishore Kumar, G., M. Venkat Ratnam, A. K. Patra, V. V. M. J. Rao, S. V. B. Rao, and D. N. Rao (2007), Climatology of low-latitude mesospheric echo characteristics observed by Indian mesosphere, stratosphere, and troposphere radar, *J. Geophys. Res.*, *112*, D06109, doi:10.1029/2006JD007609.
Kishore Kumar, G., M. Venkat Ratnam, A. K. Patra, V. V. M. Jagannadha Rao, S. Vijaya Bhaskar Rao, K. Kishore Kumar, S. Gurubaran, G. Ramkumar, and D. Narayana Rao (2008a), Low-latitude mesospheric mean winds observed by Gadanki mesosphere-stratosphere-troposphere (MST) radar and comparison with rocket, High Resolution Doppler Imager (HRDI), and MF radar measurements and HWM93, *J. Geophys. Res.*, *113*, D19117, doi:10.1029/2008JD009862.
Kishore Kumar, G., M. Venkat Ratnam, A. K. Patra, S. Vijaya Bhaskara Rao, and J. Russell (2008b), Mean thermal structure of the low-latitude middle atmosphere studied using Gadanki Rayleigh lidar, Rocket, and SABER/TIMED observations, *J. Geophys. Res.*, *113*, D23106, doi:10.1029/2008JD010511.
Kishore Kumar, G., W. Singer, J. Oberheide, N. Grieger, P. P. Batista, D. M. Riggin, H. Schmidt, and B. R. Clemesha (2014), Diurnal tides at low latitudes: Radar, satellite, and model results, *J. Atmos. Sol. Terr. Phys.*, doi:10.1016/j.jastp.2013.07.005, in press.
Kumar, K. K., G. Ramkumar, and S. T. Shelbi (2007), Initial results from SKiYMET meteor radar at Thumba (8.5°N, 77°E): 1. Comparison of wind measurements with MF spaced antenna radar system, *Radio Sci.*, *42*, RS6008, doi:10.1029/2006RS003551.
Kumar, K. K., D. Swain, S. Rachel John, and G. Ramkumar (2011), Simultaneous observations of SAO and QBO in winds, temperature and ozone in the tropical middle atmosphere over Thumba (8.5°N, 77°E), *Clim. Dyn.*, *37*, 9–10.
Kuttippurath, J., and G. Nikulin (2012), A comparative study of the major sudden stratospheric warmings in the Arctic winters 2003/2004-2009/2010, *Atmos. Chem. Phys.*, *12*, 8115–8129, doi:10.5194/acp-12-8115-2012.
Lindzen, R. S. (1981), Turbulence and stress due to gravity wave and tidal breakdown, *J. Geophys. Res.*, *86*, 9707–9714, doi:10.1029/JC086iC10p09707.
Mayr, H. G., and J. G. Mengel (2005), Inter-annual variations of the diurnal tide in the mesosphere generated by the quasi-biennial oscillation, *J. Geophys. Res.*, *110*, D10111, doi:10.1029/2004JD005055.
Pedatella, N. M., and H.-L. Liu (2013), The influence of atmospheric tide and planetary wave variability during sudden stratosphere warmings on the low latitude ionosphere, *J. Geophys. Res. Space Physics*, *118*, 5333–5347, doi:10.1002/jgra.50492.
Peña-Ortiz, C., H. Schmidt, M. A. Giorgetta, and M. Keller (2010), QBO modulation of the semiannual oscillation in MAECHAM5 and HAMMONIA, *J. Geophys. Res.*, *115*, D21106, doi:10.1029/2010JD013898.
Rajaram, R., and S. Gurubaran (1998), Seasonal variabilities of low-latitude mesospheric winds, *Ann. Geophys.*, *16*, 197–204, doi:10.1007/s00585-998-0197-4.
Ramkumar, G., T. M. Antonita, Y. Bhavani Kumar, H. Venkata Kumar, and D. Narayana Rao (2006), Seasonal variation of gravity waves in the Equatorial Middle Atmosphere: results from ISRO's Middle Atmospheric Dynamics (MIDAS) program, *Ann. Geophys.*, *24*, 2471–2480, doi:10.5194/angeo-24-2471-2006.
Ratnam, M. V., G. Kishore Kumar, B. V. K. Murthy, A. K. Patra, V. V. M. J. Rao, S. V. B. Rao, K. K. Kumar, and G. Ramkumar (2008), Long-term variability of the low latitude mesospheric SAO and QBO and their relation with stratospheric QBO, *Geophys. Res. Lett.*, *35*, L21809, doi:10.1029/2008GL035390.
Reed, R. J. (1966), Zonal wind behaviour in the equatorial stratosphere and lower mesosphere, *J. Geophys. Res.*, *71*, 4223–4233, doi:10.1029/JZ071i018p04223.
Richter, J., and R. R. Garcia (2006), On the forcing of the mesospheric semi-annual oscillation in the Whole Atmosphere Community Climate Model, *Geophys. Res. Lett.*, *33*, L01806, doi:10.1029/2005GL024378.
Rienecker, M. M., et al. (2011), MERRA: NASA's Modern-ERA Retrospective Analysis for research and Applications, *J. Clim.*, *24*, 3624–3648.
Sassi, F., and R. R. Garcia (1997), The role of equatorial waves forced by convection in the tropical semiannual oscillation, *J. Atmos. Sci.*, *54*, 1925–1942.
Sathishkumar, S., S. Sridharan, and C. Jacobi (2009), Dynamical response of low-latitude middle atmosphere to major sudden stratospheric warming events, *J. Atmos. Sol. Terr. Phys.*, *71*, 857–865, doi:10.1016/j.jastp.2009.04.002.
Smith, A. K. (2012), Global Dynamics of the MLT, *Surv. Geophys.*, *33*(6), 1177–1230, doi:10.1007/s10712-012-9196-9.
Sridharan, S., T. Tsuda, and S. Gurubaran (2007), Radar observations of long-term variability of mesosphere and lower thermosphere winds over Tirunelveli (8.7°N, 77.8°E), *J. Geophys. Res.*, *112*, D23105, doi:10.1029/2007JD008669.
Tomikawa, Y. (2010), Persistence of easterly wind during major Stratospheric Sudden Warmings, *J. Clim.*, *23*, 5258–5267, doi:10.1175/2010JCLI3507.1.
Venkateswara Rao, N., T. Tsuda, D. M. Riggin, S. Gurubaran, I. M. Reid, and R. A. Vincent (2012a), Long-term variability of mean winds in the mesosphere and lower thermosphere at low latitudes, *J. Geophys. Res.*, *117*, A10312, doi:10.1029/2012JA017850.
Venkateswara Rao, N., T. Tsuda, and Y. Kawatani (2012b), A remarkable correlation between short period gravity waves and semiannual oscillation of the zonal wind in the equatorial mesopause region, *Ann. Geophys.*, *30*, 703–710, doi:10.5194/angeo-30-703-2012.
Vincent, R. A., S. Kovalam, D. C. Fritts, and J. R. Isler (1998), Long-term MF radar observations of solar tides in the low-latitude mesosphere: Inter-annual variability and comparisons with the GSWM, *J. Geophys. Res.*, *103*, 8667–8683, doi:10.1029/98JD00482.
Xu, J., A. K. Smith, W. Yuan, H.-L. Liu, Q. Wu, M. G. Mlynczak, and J. M. Russell III (2007), Global structure and long-term variations of zonal mean temperature observed by TIMED/SABER, *J. Geophys. Res.*, *112*, D24106, doi:10.1029/2007JD008546.
Xu, J., A. K. Smith, H.-L. Liu, W. Yuan, Q. Wu, G. Jiang, M. G. Mlynczak, J. M. Russell III, and S. J. Franke (2009), Seasonal and quasi-biennial variations in the migrating diurnal tide observed by Thermosphere, Ionosphere, Mesosphere, Energetics and Dynamics (TIMED), *J. Geophys. Res.*, *114*, D13107, doi:10.1029/2008JD011298.